Chem-Bio Informatics Journal, Vol.9, pp.62-74 (2009)

Validation of Techniques for Structure Prediction and Thermostabilization of a Protein: A Case Study Using the TIM-barrel Enzyme Lactate Oxidase

Ryosuke Yamagishi[1†], Hirotaka Yagi[2], Makio Furuichi[2], Tadashi Murase[2], Hajime Ishii[2], Hiroshi Mizuno[3], Jiro Shimada[4], Hirotaka Minagawa[4], Shuhei Ohnishi[5] and Hiroki Kaneko[1*†]

[1]*Department of Integrated Sciences in Physics and Biology, College of Humanities and Sciences, Nihon University, Setagaya, Tokyo 156-8550, Japan*
[2]*VALWAY Technology Center, NEC Soft, Ltd., Tokyo 136-8627, Japan*
[3]*National Institute of Advanced Industrial Science and Technology, Tsukuba 305-8566, Japan*
[4]*Nanoelectronics Research Laboratories, NEC Corporation, Tsukuba, Ibaraki 305-8501, Japan*
[5]*Faculty of Sciences, Toho University, Funabashi, Chiba 274-8510, Japan*

**E-mail: kaneko@phys.chs.nihon-u.ac.jp*

†These authors equally contributed to this work.

(Received July 15,2009; accepted August 26,2009; published online September 15,2009)

Abstract

Recently, a variety of methods for protein structure prediction have been developed. However, there are only a limited number of studies where the results have been adequately validated. With this in mind, we have evaluated our previously predicted model of lactate oxidase by comparison with the recently determined crystal structure. In addition, we also analyzed our thermotolerant mutants that were designed on the basis of a predicted model. The validity of these procedures was assessed by comparing the results of rational design against the interpretation of the thermostabilization mechanism. Specifically, we analyzed lactate oxidase (LOX), a useful lactic acid sensor, as an example for validation. LOX was chosen because it has an $(\beta/\alpha)_8$ barrel (TIM barrel) fold, which constitutes the basic structural framework of numerous important enzymes. We also propose an effective modeling method and thermostabilization technique for the TIM barrel fold.

Key Words: homology modeling, thermostability, TIM barrel, lactate oxidase, protein engineering, biosensor, computer-aided design

Area of Interest: Bioinformatics and Bio computing

1. Introduction

Enzymes are attractive catalysts because they display many outstanding characteristics including substrate/reaction specificity as well as stereoselectivity. Accordingly, enzymes are often used for industrial processes as well as *in vivo* applications such as the manufacture of various chemicals and as biosensors for medical diagnostics. However, most proteins are highly sensitive to heat, pH and pressure, which limits their usefulness as biocatalysts. Indeed, the application of enzymes under extreme conditions is currently one of the most challenging problems to be addressed in the field of biocatalysis.

For this reason, a number of studies have been conducted to enhance thermostability of enzymes by protein engineering. In general, thermostable enzymes are screened by analyzing a number of different mutant proteins. If the three-dimensional structure of a target enzyme is already known, a thermostable version of the protein can often be obtained by rational design. However, the three-dimensional structure of a target enzyme is often unknown because protein structural studies are by no means straightforward. In such cases, prediction of the three-dimensional structure is essential for rational design of a thermostable enzyme.

The thermostabilization of enzymes using protein engineering involves three major problems. (i) The number of successful examples based on rational design is less than those that rely on a combination of random mutation and screening. This problem arises because basic theory, which can accurately estimate structural stability and activity of the enzyme, and practical calculation methodologies are not sufficiently established. (ii) Often the predictive accuracy of the three-dimensional structure is not sufficiently accurate to conduct rational design. This is especially notable with regard to the orientation of side chains, which is often important for drug/protein interactions. (iii) Even when mutants with enhanced thermostability are successfully obtained, it is often difficult to derive generic methods to obtain increased thermostabilization. Indeed, many papers do not adequately explain why the thermostability of a mutant protein is increased relative to that of wild-type. For example, most research papers tend to focus solely on the successful result of obtaining a useful mutant rather than analyzing the methodology employed in the procedure.

Here, we verify both the accuracy of our structural predictions and the techniques used for thermostabilization. Lactate oxidase (LOX), which has potential industrial applications as a lactic acid sensor, was used as the model enzyme. Moreover, LOX is also an attractive subject to study because its three-dimensional structure includes a $(\beta/\alpha)_8$ barrel (TIM barrel) fold. The group of proteins with a TIM barrel fold includes enzymes that play physiologically important functions. Indeed, the TIM barrel fold is the most common enzyme fold in the Protein Data Bank (PDB) of known protein structures [1, 2]. A three-dimensional structure of LOX monomer (single subunit) [3] as well as an enzyme-ligand complex structure and a quaternary structure [4] of LOX were predicted in our laboratory using a homology modeling technique. Furthermore, various LOX mutants with enhanced thermostability have been produced and reported in our laboratory using techniques such as rational design [4], random mutagenesis [5] and directed evolution [6].

Recently, three research groups including ourselves clarified the three-dimensional structure of LOX using X-ray crystal structure analysis [7][8][9]. In this paper, the correct structure and predicted model structure are compared, and the accuracy of our modeling method is evaluated. In addition, the rationale used for increased thermostabilization is examined using the known crystal structure of the enzyme. Finally, we attempted to derive a versatile method for enzyme thermostabilization based on these findings.

2. Materials and methods

2.1 Homology modeling method

We have proposed a novel homology modeling method that aims to enhance the prediction accuracy by focusing on the highly conserved hydrophobic core and making maximum use of the available information. For example, the amino acids making up the hydrophobic core, which are considered to be structurally well-conserved during evolution, are automatically extracted on the basis of the three dimensional structure of the reference protein. The hydrophobic core score is then calculated for each residue. The higher the score, the deeper the residue is located within the hydrophobic core. Use of the core scores in the alignment procedure reduces the number of gaps in the hydrophobic core region. This is because matching up specific residues from the target protein to a core residue from the reference protein is given high priority. It has already been shown that this method gives more reliable alignment for homology modeling than conventional methods. Moreover, hydrophobic core distance (HCD), which is a pseudo-distance defined for each residue of the reference protein using the core score system, is also calculated. If HCD of a certain residue is large, it means that the residue is very likely to locate near the solvent accessible surface (i.e., far from the hydrophobic core) and belong to insertion/deletion sites. The introduction of the concept of HCD has made a substantial contribution to generating better predictions of insertion/deletion sites, and hence to a more accurate prediction of structural differences around these sites (see our previous paper [10] for details). To evaluate our model and the accuracy of our modeling procedure, Modeller 9v1 [11] was used for the modeling of lactate oxidase (LOX). The modeling process was conducted using the crystal structure of glycolate oxidase (PDB ID:1GOX) [12] as the same template and Discovery Studio 2.1 (Accelrys Inc.) as an interface. Subsequently, orientation of side chains was optimized using a side-chain prediction program, SCWRL3.0 [13]. All figures were drawn using Discovery Studio 2.1.

2.2 Comparison of the three-dimensional structures

Fitting was performed using the McLachlan algorithm [14] as implemented in the program ProFit [15]. Root Mean Square Distance (RMSD) was calculated between Cα atoms, side chains, and all heavy atoms based on the results of the fitting. In addition, the main chain and especially the position of the Cα atoms were estimated using MaxSub, which evaluates the quality of predicted protein structure models [16]. The MaxSub score is calculated from the distance between Cα atoms in a model structure and the experimentally determined structure; as the distance decreases the score value is increased. Therefore, more accurate models give a larger MaxSub score.

2.3 Structure prediction of mutants

Mutant models were generated using Discovery Studio 2.1. CHARMm force field was allocated to the model. On applying the Generalized Born approximation, molecular mechanics (MM) was carried out. The coordinates of only the crystallographic waters were refined by 200 steps of energy minimization using steepest descent method (SD), followed by 200 steps of minimization for the crystallographic waters and side chains of the mutant model. This procedure was then followed by 500 steps using SD and 500 steps using conjugate gradient method (CG) for all atoms.

2.4 Structure prediction of the LOX-substrate (L-lactic acid) complex

L-lactic acid was manually superimposed on a crystal structure of LOX binding with D-lactic acid (PDB ID:2NLI) [7]. CHARMm force field was allocated to the structure. On applying the Generalized Born approximation, MM was carried out. The coordinates of the crystallographic waters and L-lactic acid were refined by 200 steps of energy minimization using SD, followed by 200 steps of minimization for the crystallographic waters, L-lactic acid and side chains of the mutant model. This process was then followed by 500 steps using SD and 500 steps using CG for all atoms.

3. Results and discussion

3.1 Predictive accuracy of the modeling

First, modeled lactate oxidase (LOX) single subunit was compared between a predicted model structure [3] and a crystal structure (PDB ID:2J6X) [9] (Figure 1A). As anticipated from the amino acid sequence, the basic skeleton of LOX forms a TIM barrel fold. Indeed, FMN-dependent α-hydroxy acid oxidase family enzymes requiring FMN (flavin mononucleotide) frequently adopt a TIM barrel fold in their functionally important domain. The three-dimensional structure of several members of this family of proteins have been determined, including glycolate oxidase (GOX) [12], FMN-binding domain of flavocytochrome b_2 (FCB) [17], mandelate dehydrogenase (chimeric mutant in which residues 177-215 of mandelate dehydrogenase are replaced by residues 176-195 of GOX from spinach) (MDH) [18], long chain α-hydroxy acid oxidase (LCHAO) [19] as well as LOX. As shown in Figure 1A, the structure of the main chain was accurately predicted throughout (RMSD for Cα atoms = 2.215), but loops at the surface and the N- and C-terminal regions differ between prediction and the known structure. In particular, a major difference was observed in a large loop called the barrel loop 4 (Ala173-Ile222 in lactate oxidase), situated between β-strand 4 and α-helix 4 of the TIM barrel [19]. However, accurate comparison of static structures may have little value because the structure of loop 4 varies greatly in different crystal structures. For example, loop 4 in two crystal structures formed under different crystallization conditions (PDB IDs: 2J6X and 2NLI) have different structures. Furthermore, even in the same crystal, each subunit adopts a different structure (e.g., A chain and D chain of 2J6X). Based on these considerations and data of temperature factors, loop 4 is presumed to possess high mobility. Therefore it is most likely that accurate comparison of static structures of this part of the molecule may have little value.

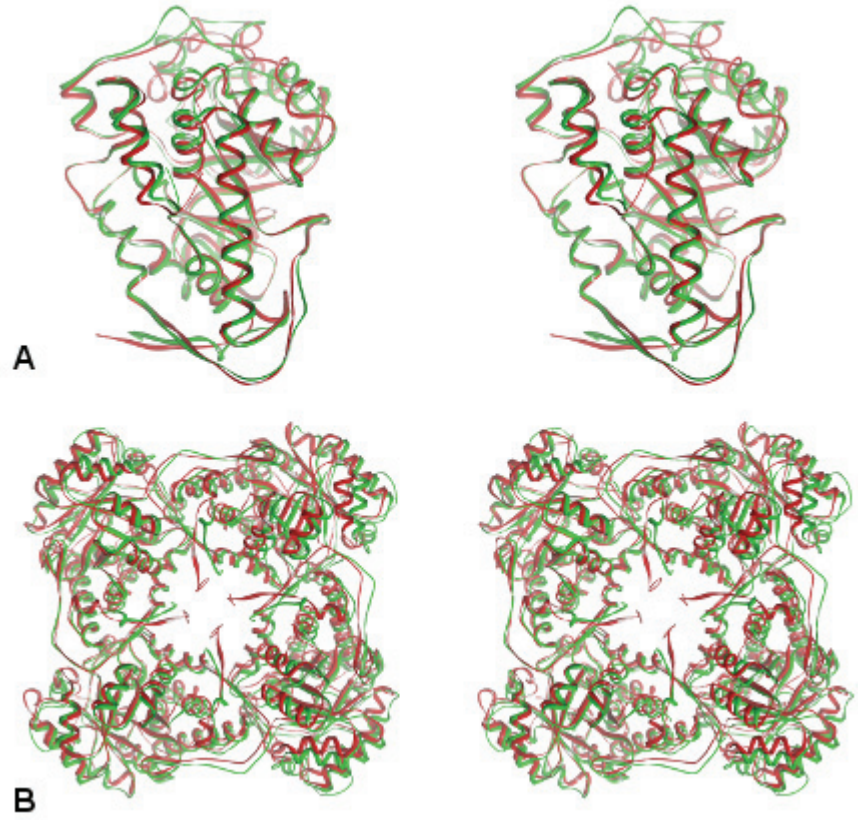

Figure 1. Comparison of the LOX main chain between our model and a crystal structure of the protein (with stereo imagery).
Green solid ribbon and red solid ribbon represent our model and the crystal structure [9] (PDB ID:2J6X Chain A), respectively. (A) Monomer. (B) Tetramer forming the quaternary structure.

For quaternary structure, our previously predicted structure [4] and a crystal structure were also compared. The relative orientation of the four subunits in the predicted and experimentally determined structures was found to be in very good agreement (Figure 1B).

Next, we verified the accuracy of the protein structure prediction. The result of this analysis is summarized in Table 1. Sequence identity between LOX and a template [glycolate oxidase (GOX) [12]] used for homology modeling was 32%. It is known that homology modeling accuracy generally indicates an average predictive accuracy (i.e., value shown in the rightmost column of Table 1 [20]) when the sequence identity between a template protein and a predicted protein is about 30%. However, there is a difference in the modeling accuracy depending on the programs used. Our prediction results indicate a much higher accuracy value for Cα (main chain), side chain and all atoms than any average predictive accuracy obtained using well-known programs. Indeed, the algorithm used in our homology modeling method [10] incorporates several strategies for increasing predictive accuracy e.g., use of a hydrophobic core score system and hydrophobic core distances (see *Materials and Methods*). Nevertheless, the improvement in predictive accuracy of our methodology is better than anticipated. It is noteworthy that the values used for the comparison of the accuracy represent average predictive accuracies of proteins with various folding structures that share ~30% sequence identity. It can be hypothesized that within a given folding pattern, such as a TIM barrel fold, homology modeling accuracy is higher than average. To verify this hypothesis, LOX structure was predicted under a similar condition using Modeller 9v1 [11], which is one of the

most popular modeling software programs. As shown in Table 1, predictive accuracy obtained from our method was equivalent or better than the result obtained from the Modeller 9v1. In particular, there were notable difference in RMSD values of the main chains and overall (all atoms) structure. However, prediction based on Modeller 9v1 followed by side-chain re-prediction using SCWRL indicated slightly better results in terms of orientation of side chains than the prediction result based on our original method. This observation indicates that the prediction of side chain conformation by SCWRL is excellent and that this program is highly useful [20]. Thus, this result suggests that predictive accuracy would increase in proteins with a folding pattern that has a considerably limited shape over the entire molecule regardless of the prediction method.

Table 1. Predictive accuracies of model structures of chain A in PDB ID:2J6X was used as the correct structure here.

[a]Average predictive accuracy at sequence identity (≈30 %) [20].

[b]Fraction of side-chain dihedral angles, $\chi 1$ and $\chi 2$, that where within 30 degrees from the angles in the correct structure.

		Our Model	Modeller	Modeller&SCWRL	Average predictive accuracy[a]
Cα					
	RMSD (Å)	2.215	2.763		3.0~4.5
	MaxSub	0.875	0.888		0.6~0.7
side –chain					
	correct $\chi 1$[b]	60.8%	58.9%	65.4 %	
	correct $\chi 2$[b]	46.8%	51.7%	60.7 %	
	correct $\chi 1$ & $\chi 2$[b]	54.7%	55.8%	63.4 %	25~40 %
all atoms					
	RMSD (Å)	3.002	3.431	3.427	4.0~4.5

Despite recent advances in X-ray crystallographic techniques, experimental determination of a protein structure remains highly challenging. For example, we studied LOX for more than 10 years before we succeeded in clarifying its crystal structure. Given the urgent need for biocatalysts in medical and industrial applications, it is not practical to placing too much importance on elucidation of the three-dimensional structure before initiating a program of molecular design. Accordingly, molecular design based on predicted structure, rather than an experimentally determined structure, offers a more pragmatic approach. Therefore, we suggest the following strategies. For structure prediction of proteins made up of a combination of similar folding patterns throughout the entire molecule, such as a TIM barrel fold, “purpose-built” modeling methods specialized for each structural pattern should be used. Such specialized modeling methods involve the following steps: first, each folding pattern is comprehensively analyzed, and moieties that readily form common structures are extracted. This extraction should be done by dividing proteins into “subgroups” having a similar structure and function. The structures are then separately extracted from each “subgroup”, rather than simply extracting from the entire array of protein structures displaying the same folding pattern. Then, each amino acid, which has a tendency to locate at the residual position with a specific orientation of the side chain, is scored according to position-specific definitions. Use of these scoring systems, referred to as the restricted threading method, reflect a more detailed structure of the subgroup in a folding pattern. A combination of the usual homology modeling method and this restricted threading method enhances the predictive accuracy for both the main chain and side chains of the protein.

3.2 Validation of the thermostabilization technique and its rational

Here, two LOX mutants selected from our array of mutant proteins, which had gained thermostability as previously reported, were analyzed using the crystal structure or the mutant model derived from it. The two mutants were E303Q [4], which was obtained by rational design based on a predicted structure, and E160G/V198I/G36S/T103S/A232S/F277Y [6], which was obtained by directed evolution.

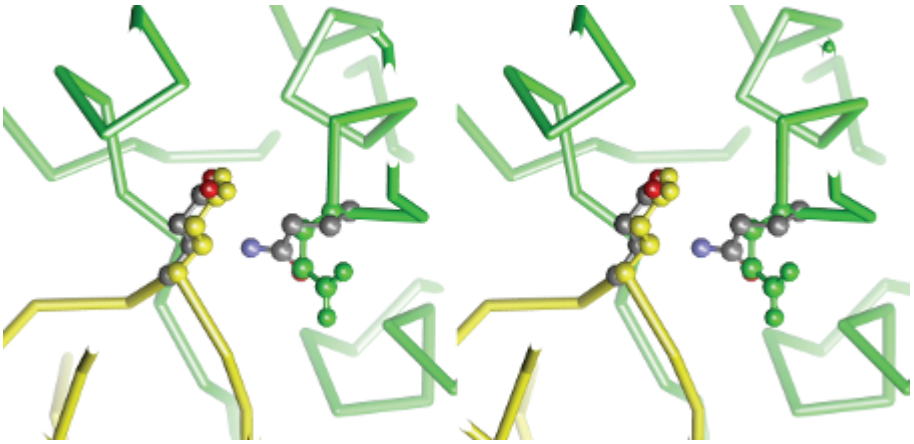

Figure 2. Structures around the subunit interface in the wild-type and E303Q mutant (with stereo imagery).
Main chain and a side chain of Glu 303 of one of the wild-type subunits are indicated in green. Main chain and a side chain of Glu 272 of adjacent subunit of the wild type are indicated in yellow. Side chains of Glu 303 and Glu 272 of the mutant are indicated by atom types in different colors (carbon, grey; oxygen red; nitrogen, blue).

E303Q mutant

This mutant was designed using a deductive approach based on a predicted structure with the aim of stabilizing its quaternary structure by strengthening interaction between the subunits. Based on a predicted LOX model, Glu 272 and Glu 303 are located at the interface between each subunit, which presumably undergo electrostatic repulsion. Therefore, a mutant protein was generated in which one of the residues (Glu 303) was substituted with Gln in order to hinder dissociation of the subunits and further strengthen intersubunit interaction by hydrogen bonding.

To verify whether this design strategy was useful, E303Q mutant model was generated based on a crystal structure and compared with the wild-type crystal structure (Figure 2). In the crystal structure of the wild-type enzyme, Glu 303 and Glu 272 on the adjacent subunit are located about 6.1 Å apart. By contrast, in the mutant protein Gln 303, corresponding to Glu 303 of the wild-type enzyme, is positioned only 5.0 Å from Glu 272 on the adjacent subunit. From these results, we concluded that the mutant protein had acquired thermostability through strengthened interaction between subunits based largely on the expected rationale.

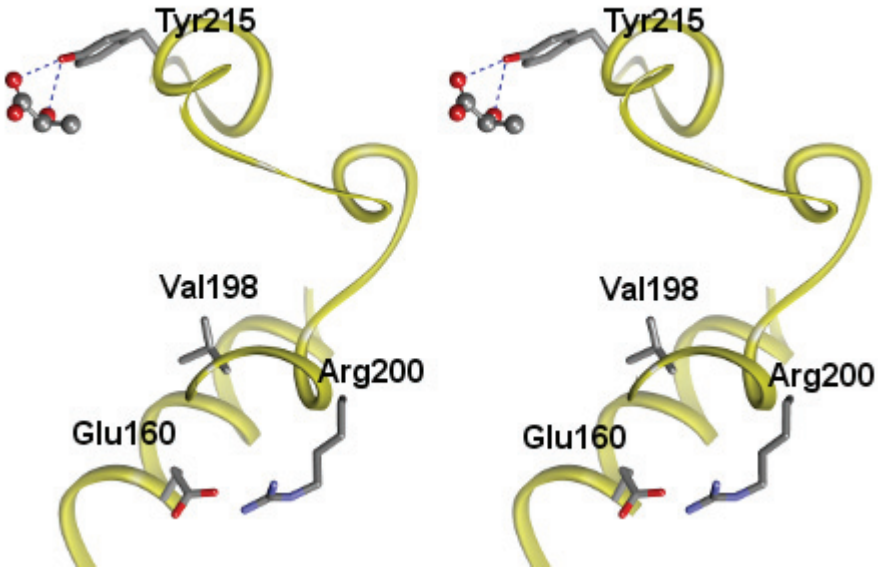

Figure 3. Structure around loop 4 in a model of the wild type LOX and substrate (L-lactic acid) complex (with stereo imagery).
Main chain and L-lactic acid are indicated with yellow solid ribbon, and balls and sticks, respectively. Side chains of Glu 160, Val 198, Arg 200 and Tyr 215 are indicated as sticks. Dotted lines represent hydrogen bonds.

E160G/V198I/G36S/T103S/A232S/F277Y mutant

It is already known that coexistence of E160G and V198I mutations act in a concerted fashion, rather than additively, to enhance thermostability of the protein [5]. However, this mechanism cannot be easily reconciled from observations of the known structure of the enzyme. Analysis of the structure suggests that mutations E160G and V198I will specifically influence loop 4 (a loop between β-strand 4 and α-helix 4) or residues 190-220, which form part of the loop. Loop 4 has a structure like a lid covering the active site. Tyr 215 is located in this loop and is predicted to bind with the substrate. Nonetheless, Tyr 215 is not conserved in other enzyme families. Therefore, it is expected that the loop 4, especially Tyr 215 located in the loop, is the site providing specificity of LOX [9]. Glu 160 forms a salt bridge with Arg 200 in loop 4, and Val 198 is also located within the loop (Figure 3). It is thought that the E160G mutation breaks the salt bridge between Glu 160 and Arg 200, thereby increasing flexibility of the loop and facilitating the opening of the lid covering the active site. Thus, although substrate can readily access the active site, increased mobility of the lid causes instability of the protein structure. To eliminate this problem, V198I mutation was also introduced. It was anticipated that this additional mutation would increase hydrophobic packing inside of the molecule, thereby increasing both stability and activity. Given the importance of the balance between structural stability and flexibility of enzyme function [21], simultaneous introduction of both E160G and V198I mutations was fully anticipated to act in concert, rather than in an additive fashion, to enhance thermostability of the protein structure.

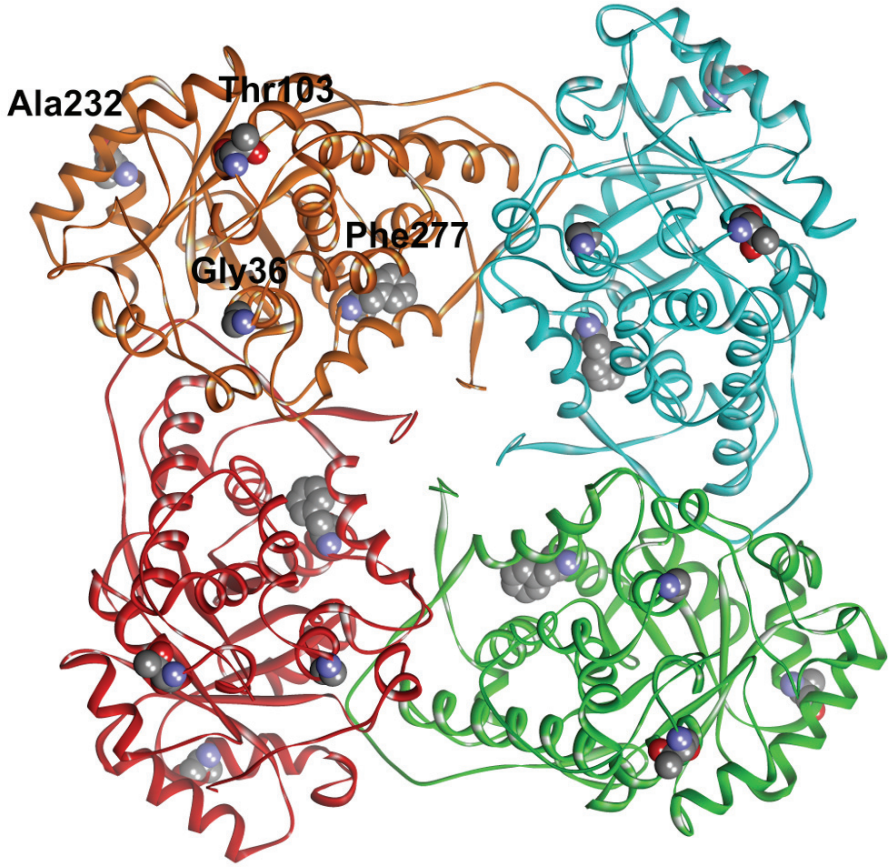

Figure 4. Location of mutations in the crystal structure (PDB ID:2J6X) of LOX (quaternary structure).
Main chains of each subunit are indicated as solid ribbons in different colors, and mutated residues Gly 36, Thr 103, Ala 232 and Phe 277 are indicated in a CPK model.

Using the above E160G/V198I mutant, E160G/V198I/G36S/T103S/A232S/F277Y mutant was obtained by directed evolution [6]. This mutant has further improved thermostability as compared with the E160G/V198I mutant, and displays the highest LOX thermostability among the previously identified mutants in our laboratory. Observation of the crystal structure of LOX reveals that none of the six residues 36, 103, 160, 198, 232 and 277 are located at positions of interaction between adjacent subunits. Therefore, it is presumed that any mutations in these residues do not directly contribute to stabilization of the protein quaternary structure. Indeed, this conclusion is consistent with preliminarily predictions based on the wild-type model structure. Meanwhile, examination of the other four mutated sites, with the exception of residues 160 and 198, revealed the following observations. First, side chains of residues 36, 103, 232 and 277 were all solvent exposed (Figure 4). These four mutated sites were also substituted by residues with greater hydrophilicity. In addition, despite the hydrophobic nature of the side chain, Phe277 is exposed on the protein surface (Figure 5A), which is entropically disadvantageous. Observations of the mutant model suggest that a change to Tyr in this position enables the residue to form hydrogen bonds more readily with nearby amino acids or surrounding water molecules (Figure 5B). Accordingly, results of these additional four mutations introduced by directed evolution agree with the observation that stability of the

protein is enhanced by substitution of amino acids exposed on the protein surface with those of increased hydrophilicity [22]. It is unclear, however, whether this rule can be applied more generally [23].

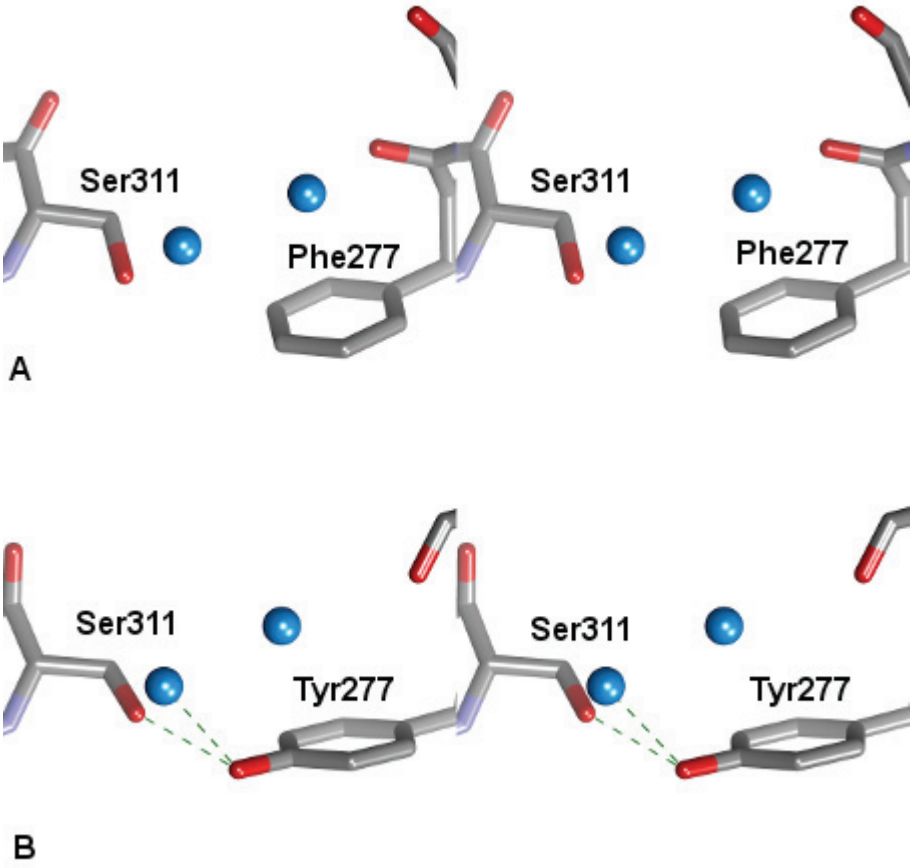

Figure 5. Structural comparison around a mutated residue 277 with stereo imagery.
Water molecules are indicated as spheres in cyan. (A) Wild-type (Phe 277), (B) Mutant (Tyr 277). Dotted line represents hydrogen bonds.

To address this point, we analyzed amino acid type and solvent accessibility of the side chains of residues 36, 103, 232 and 277 using four other proteins belonging to the FMN-dependent α-hydroxy acid oxidase family (Table 2). Solvent accessibility represents solvent accessible surface (SAS) area in $Å^2$. SAS was calculated using a DCLM method [24]. The analysis indicated that in other proteins amino acids corresponding to Thr 103 and Ala 232 of wild-type LOX were hydrophilic and their side chains were exposed to solvent. Thus, it can be concluded that T103S and A232S mutations contribute to enhanced stability *via* the same mechanism used by other proteins within the family. Furthermore, a site corresponding to Phe 277 of wild-type LOX in other family members is occupied by a hydrophobic amino acid that is buried within the protein milieu. By contrast, Phe277 of LOX is slightly exposed to solvent at the protein surface. Therefore, we can conclude that the F277Y mutation confers a beneficial effect by stabilizing the structure of LOX. The site corresponding to Gly 36 of wild-type LOX has also been analyzed. No clear commonality difference among the family members in terms of hydrophobicity and degree of burial of the side

chain at this position could be discerned. However, the general concept that substitution of a surface exposed residue by a more hydrophilic amino acid results in enhanced protein stability seems to be correct. Certainly, this idea is applicable to the thermostabilization of members of the FMN-dependent α-hydroxy acid oxidase family of proteins that have a TIM barrel fold.

Table 2. Mutation sites in lactate oxidase and the corresponding sites in the family.
GOX, glycolate oxidase (PDB ID: 1GOX [12]); FCB, FMN-binding domain of Flavocytochrome b_2 (1FCB [17]); LCHAO, long-chain hydroxy acid oxidase (1TB3 [19]); MDH, mandelate dehydrogenase (1P4C [18]).

mutant LOX	36 Ser	103 Ser	232 Ser	277 Tyr
wild LOX	36 Gly	103 Thr	232 Ala	277 Phe
side-chain solvent accessibili($Å^2$)	14.089	38.178	41.261	1.510
GOX	20 Met	87 Glu	221 Thr	266 Ile
side-chain solvent accessibility	53.873	77.187	70.557	0.000
FCB	139 Gln	207 Glu	340 Lys	385 Ile
side-chain solvent accessibility	3.426	51.876	91.711	0.000
LCHAO	19 Thr	86 Asp	214 Ser	259 Ile
side-chain solvent accessibility	11.980	45.870	40.430	0.000
MDH	22 Met	89 Lys	222 Asp	267 Met
side-chain solvent accessibility	66.887	83.846	97.818	0.000

4. Conclusion

Both residues 103 and 232 of LOX are located in one of eight important helices comprising a TIM barrel. Accordingly, we hypothesize that thermostability can be achieved by substituting residues that fulfill the following three criteria with an amino acid of greater hydrophilicity; specifically the target residue should be i) located in one of eight important helices comprising a TIM barrel, ii) exposed at the protein surface, and iii) must not participate in any interaction beneficial to thermostabilization. To validate this hypothesis, we examined the type of amino acid occupying the position corresponding to residues 103 and 232 of wild-type LOX in the TIM-barrel enzymes from a hyperthermophilic archaeon by rigorous superposition of the three-dimensional structure using the DaliLite-pairwise option (*version 3.1*) [25]. For example, it was confirmed that several enzymes, including tryptophan synthase α-subunit from *Pyrococcus furiosus* (PDB ID: 1GEQ) [26] and the tetrameric hyperthermostable triosephosphate isomerase from *Pyrococcus woesei* (PDB ID: 1HG3) [27], have highly hydrophilic amino acids located in these positions. However, herein are described results from a preliminary analysis and further comprehensive studies are required to obtain conclusive evidence as to whether the proposed hypothesis for thermostabilization can be expanded to include all enzymes containing a TIM barrel fold. The results of this analysis will be published elsewhere.

References

[1] R. K. Wierenga, The TIM-barrel fold: a versatile framework for efficient enzymes, *FEBS Lett.*, **492**, 193-8 (2001).

[2] H. Hegyi and M. Gerstein, The relationship between protein structure and function: a comprehensive survey with application to the yeast genome, *J. Mol. Biol.*, **288**, 147-64 (1999).

[3] H. Kaneko, H. Minagawa, N. Nakayama, S. Nakamoto, S. Handa, J. Shimada, T. Takada and H. Umeyama, Modeling study of a lactate oxidase-ligand complex: Substrate specificity and thermostability, *Res. Commun. Biochem. Cell. Mol. Biol*, **2**, 234-244 (1998).

[4] H. Kaneko, H. Minagawa and J. Shimada, Rational design of thermostable lactate oxidase by analyzing quaternary structure and prevention of deamidation, *Biotechnol. Lett.*, **27**, 1777-84 (2005).

[5] H. Minagawa, J. Shimada and H. Kaneko, Effect of mutations at Glu160 and Val198 on the thermostability of lactate oxidase, *Eur. J. Biochem.*, **270**, 3628-33 (2003).

[6] H. Minagawa, Y. Yoshida, N. Kenmochi, M. Furuichi, J. Shimada and H. Kaneko, Improving the thermal stability of lactate oxidase by directed evolution, *Cell Mol. Life Sci.*, **64**, 77-81 (2007).

[7] M. Furuichi, N. Suzuki, B. Dhakshnamoorhty, H. Minagawa, R. Yamagishi, Y. Watanabe, Y. Goto, H. Kaneko, Y. Yoshida, H. Yagi, I. Waga, P. K. Kumar and H. Mizuno, X-ray structures of *Aerococcus viridans* lactate oxidase and its complex with D-lactate at pH 4.5 show an α-hydroxyacid oxidation mechanism, *J. Mol. Biol.*, **378**, 436-46 (2008).

[8] Y. Umena, K. Yorita, T. Matsuoka, A. Kita, K. Fukui and Y. Morimoto, The crystal structure of L-lactate oxidase from *Aerococcus viridans* at 2.1 Å resolution reveals the mechanism of strict substrate recognition, *Biochem. Biophys. Res. Commun.*, **350**, 249-56 (2006).

[9] I. Leiros, E. Wang, T. Rasmussen, E. Oksanen, H. Repo, S. B. Petersen, P. Heikinheimo and E. Hough, The 2.1 Å structure of *Aerococcus viridans* L-lactate oxidase (LOX), *Acta Crystallogr. Sect. F Struct. Biol. Cryst. Commun.*, **62**, 1185-90 (2006).

[10] H. Kaneko, T. Kuriki, J. Shimada, S. Handa, H. Takata, M. Yanase, S. Okada, T. Takada and H. Umeyama, Modeling Study of the Neopullulanase-Maltoheptaose Complex, *Res. Commun. Biochem. Cell. Mol. Biol*, **2**, 37-54 (1998).

[11] A. Šali, Comparative protein modeling by satisfaction of spatial restraints, *Mol. Med. Today*, **1**, 270-7 (1995).

[12] Y. Lindqvist, Refined structure of spinach glycolate oxidase at 2 Å resolution, *J. Mol. Biol.*, **209**, 151-66 (1989).

[13] A. A. Canutescu, A. A. Shelenkov and R. L. Dunbrack, Jr., A graph-theory algorithm for rapid protein side-chain prediction, *Protein. Sci.*, **12**, 2001-14 (2003).

[14] A. D. McLachlan, Rapid comparison of protein structures, *Acta Crystallogr. A.*, **38**, 871-873 (1982).

[15] ProFit (URL=http://www.bioinf.org.uk/software/profit)

[16] N. Siew, A. Elofsson, L. Rychlewski and D. Fischer, MaxSub: an automated measure for the assessment of protein structure prediction quality, *Bioinformatics*, **16**, 776-85 (2000).

[17] Z.-x. Xia and F. S. Mathews, Molecular structure of flavocytochrome b2 at 2.4 Å resolution, *J. Mol. Biol.*, **212**, 837-63 (1990).

[18] N. Sukumar, A. R. Dewanti, B. Mitra and F. S. Mathews, High resolution structures of an oxidized and reduced flavoprotein. The water switch in a soluble form of (S)-mandelate dehydrogenase, *J. Biol. Chem.*, **279**, 3749-57 (2004).

[19] L. M. Cunane, J. D. Barton, Z. W. Chen, K. H. Le, D. Amar, F. Lederer and F. S. Mathews, Crystal structure analysis of recombinant rat kidney long chain hydroxy acid oxidase, *Biochemistry*, **44**, 1521-31 (2005).
[20] B. Wallner and A. Elofsson, All are not equal: a benchmark of different homology modeling programs, *Protein. Sci.*, **14**, 1315-27 (2005).
[21] P. A. Fields, Review: Protein function at thermal extremes: balancing stability and flexibility, *Comp. Biochem. Physiol. A Mol. Integr. Physiol.*, **129**, 417-31 (2001).
[22] C. Strub, C. Alies, A. Lougarre, C. Ladurantie, J. Czaplicki and D. Fournier, Mutation of exposed hydrophobic amino acids to arginine to increase protein stability, *BMC Biochem.*, **5**, 9 (2004).
[23] S. Kumar and R. Nussinov, How do thermophilic proteins deal with heat?, *Cell Mol. Life Sci.*, **58**, 1216-33 (2001).
[24] F. Eisenhaber, P. Lijnzaad, P. Argos, C. Sander and M. Scharf, The double cubic lattice method: efficient approaches to numerical integration of surface area and volume and to dot surface contouring of molecular assemblies, *J. Comput. Chem.*, **16**, 273-84 (1995).
[25] L. Holm and J. Park, DaliLite workbench for protein structure comparison, *Bioinformatics*, **16**, 566-7 (2000).
[26] Y. Yamagata, K. Ogasahara, Y. Hioki, S. J. Lee, A. Nakagawa, H. Nakamura, M. Ishida, S. Kuramitsu and K. Yutani, Entropic stabilization of the tryptophan synthase α-subunit from a hyperthermophile, *Pyrococcus furiosus*. X-ray analysis and calorimetry, *J. Biol. Chem.*, **276**, 11062-71 (2001).
[27] H. Walden, G. S. Bell, R. J. Russell, B. Siebers, R. Hensel and G. L. Taylor, Tiny TIM: a small, tetrameric, hyperthermostable triosephosphate isomerase, *J. Mol. Biol.*, **306**, 745-57 (2001).